ORIGINAL ARTICLE OPEN ACCESS

Have We Selected for Higher Mesophyll Conductance in Domesticating Soybean?

Elena A. Pelech[1,2] | Samantha S. Stutz[2] | Yu Wang[3] | Edward B. Lochocki[2] | Stephen P. Long[1,2,4]

[1]Department of Plant Biology, University of Illinois at Urbana-Champaign, Urbana, Illinois, USA | [2]Carl R Woese Institute for Genomic Biology, University of Illinois at Urbana-Champaign, Urbana, Illinois, USA | [3]School of Life Sciences, Nanjing University, Nanjing, China | [4]Department of Crop Sciences, University of Illinois at Urbana-Champaign, Urbana, Illinois, USA

Correspondence: Elena A. Pelech (pelech@illinois.edu) | Stephen P. Long (slong@illinois.edu)

ABSTRACT

Soybean (*Glycine max*) is the single most important global source of vegetable protein. Yield improvements per unit land area are needed to avoid further expansion onto natural systems. Mesophyll conductance (g_m) quantifies the ease with which CO_2 can diffuse from the sub-stomatal cavity to Rubisco. Increasing g_m is attractive since it increases photosynthesis without increasing water use. Most measurements of g_m have been made during steady-state light saturated photosynthesis. In field crop canopies, light fluctuations are frequent and the speed with which g_m can increase following shade to sun transitions affects crop carbon gain. Is there variability in g_m within soybean germplasm? If so, indirect selection may have indirectly increased g_m during domestication and subsequent breeding for sustainability and yield. A modern elite cultivar (LD11) was compared with four ancestor accessions of *Glycine soja* from the assumed area of domestication by concurrent measurements of gas exchange and carbon isotope discrimination ($\Delta^{13}C$). g_m was a significant limitation to soybean photosynthesis both at steady state and through light induction but was twice the value of the ancestors in LD11. This corresponded to a substantial increase in leaf photosynthetic CO_2 uptake and water use efficiency.

1 | Introduction

Soybean (*Glycine max* [L.] Merr.) is among the most important agricultural seed crops globally as the largest single source of vegetable protein and the second largest source of vegetable oils. The major areas of production are North and South America, and eastern Asia (Specht et al. 2014; Anderson et al. 2019). Improved agronomic practices and intensive breeding programmes have resulted in sustained soybean yield increases. However, these have not been sufficient to satisfy increasing demand which has resulted in expansion onto more natural land (Specht et al. 2014; Anderson

et al. 2019; Williams et al. 2021). Increasing photosynthetic efficiency, especially if this can be achieved without more water, may be one way to supplement breeding efforts and achieve more yield within existing land of cultivation (Burgess et al. 2023; Long, Marshall-Colon, and Zhu 2015; Murchie, Pinto, and Horton 2009). In an agricultural setting, crop canopy leaves consistently experience light intensity fluctuations due to changing solar angles, cloud cover, wind and intraspecific shading (Pearcy 1990; Long et al. 2022). Soybean is also a common understory legume crop in intercropping systems where such light fluctuations are intensified by interspecific shading (Adeniyan and Ayoola 2006; Kamara

et al. 2019; Li et al. 2020; Mbah, Muoneke, and Okpara 2009; Pelech, Alexander, and Bernacchi 2021; Pelech et al. 2023). However, the response of photosynthesis to fluctuating light is not instant and the resulting loss may cost up to 13% of potential carbon assimilation in soybean (Wang et al. 2020). Exploring the factors limiting photosynthesis under both dynamic and steady-state light conditions may aid a sustainable improvement of soybean productivity.

Leaf photosynthetic CO_2 assimilation (A) shows a slow rise or induction on shade to sun transitions before reaching steady state. Both induction and steady-state photosynthesis can each be limited by (1) conductance of CO_2 from the air around the leaf to the site of assimilation in the chloroplast, (2) the maximum rate of ribulose 1,5-biphosphate (RuBP) carboxylation (V_{cmax}) and (3) electron transport rate for the regeneration of RuBP (J). The CO_2 diffusion path is characterised by two spatially sequential components, stomatal conductance (g_s) and mesophyll conductance (g_m). The path from the leaf boundary layer to the intercellular airspaces across the stomata defines g_{sw}, whereas g_m in C_3 crops is the gas to liquid phase CO_2 diffusion path between leaf intercellular airspaces to Rubisco within the chloroplast stroma of the mesophyll cells (Flexas et al. 2008). Across studies and crop species, significant variations in the speed of stomatal opening during light induction exist (Acevedo-Siaca et al. 2020; De Souza et al. 2020; Long et al. 2022), limiting photosynthetic rates between 10% and 15% (McAusland et al. 2016). On the other hand, the understanding of the limitation imposed by g_m to A during induction and steady state has rarely been evaluated due to greater difficulty of estimating g_m, especially under dynamic light conditions (Leverett and Kromdijk 2024; Salesse-Smith, Driever, and Clarke 2022).

The response of g_m to shade to sun transitions has been quantified using two techniques: (1) combined measurements of gas exchange and chlorophyll fluorescence or (2) simultaneous measurements of gas exchange with carbon isotope discrimination ($\Delta^{13}C$). Kaiser et al. (2017) used the 'Variable J' method (Harley et al. 1992) with the former technique. The study refrained from quantifying the limitation to A during induction due to the assumptions and estimation bias with the Variable J method, but the steady-state values compared well to other techniques (Bernacchi et al. 2002; Flexas et al. 2008; von Caemmerer and Evans 2015). Using the $\Delta^{13}C$ technique has been suggested a more accurate method of estimating g_m due to the high sensitivity and specificity of tunable-diode laser (TDL) absorption spectroscopy (Flexas et al. 2018; Leverett and Kromdijk 2024). A mechanistic model has been used to determine g_m under dynamic conditions that relates $\Delta^{13}C$ to the multiple carbon isotope fractionation events. This utilizes the different speeds at which the two CO_2 isotopologues ($^{12}CO_2$ and $^{13}CO_2$) diffuse and/or are processed in biochemical reactions. This technique was used to measure g_m in Arabidopsis and tobacco under non-photorespiratory conditions by Sakoda et al. (2021) who found that the limitation of g_m to A was the smallest compared to the limitations imposed by g_{sw}, V_{cmax} and J through induction. However, Liu et al. (2022) used the same technique in two Arabidopsis lines and found the relative limitation g_m imposed on A during induction was > 35%. Liu et al. (2022) also re-analysed the limitation data presented in Sakoda

et al. (2021) by time integration and found a > 20% g_m limitation on A during induction.

Whether g_m imposes a significant limitation to A during light induction and/or at steady state in soybean remains to be explored. Soybean was domesticated from *Glycine soja* [Siebold & Zucc] in China 6000–9000 years ago (Kim et al. 2012) which is a vining plant that would have escaped much shade compared to the considerable self-shading and sun-flecking that occurs in today's dense soybean crop canopies, which can have a leaf area index of over six (Dermody, Long, and DeLucia 2006). In selecting for higher yield or water use efficiency, indirect selection for higher g_m could be expected if there is variation in g_m within the germplasm. Determining whether variation exists is key to understanding if there is sufficient variation to allow for direct breeding selection for increased g_m, and in turn increased productivity and water use efficiency (Specht et al. 2014; Anderson et al. 2019). This study tests the question of whether during domestication and subsequent breeding an inadvertent selection for increased g_m occurred, given its pivotal role in both crop photosynthetic efficiency and use of water. The hypotheses tested are: (1) g_m is a significant limitation to soybean photosynthesis both during light induction and at steady state and (2) domestication and selection have both increased g_m, corresponding with increased leaf photosynthesis and water use efficiency.

2 | Methods and Materials

2.1 | Accession Selection

Ancestral soybean accessions *G. soja* [Siebold & Zucc] were selected from the U.S. National Plant Germplasm System (https://npgsweb.ars-grin.gov/gringlobal/search). The *G. soja* accessions were chosen from locations in the assumed regions of N.E. China where the germplasm, subsequently introduced into N. America, was domesticated (Liu et al. 2020). Four such accessions in maturity groups II through IV were selected (Table 2). The domesticated high-yielding elite cultivar LD11-2170 of *G. max* [L.] Merr was used for comparison.

2.2 | Growth Conditions

To allow imbibition, the seed coats of ancestral accessions were cut, and the seed placed on wet paper towels for 1 week before sowing. Accessions were sown on 15 April 2022, at the University of Illinois Champaign-Urbana in pots of 0.1 m depth filled with germination growing medium (Cultivation Nation Seventy Thirty Growing Media, Fox Farm, USA). Four to six seedlings of each accession were then transplanted after 7–10 days into 6-L pots filled with the same growing medium as for germination but supplemented with 30 mL of slow-release fertiliser (Osmocote Plus 15-9-12, ICL-US). Once the ancestral accessions had established in the 6-L pots, a 1 m wire tomato cage was inserted to each pot support tendril development (Supporting Information S1: Figure 1B). LD-11-2170 was grown alongside the ancestral accessions. Plants were watered twice

daily. The average temperature of the greenhouse was 29.2°C with a 14-h photoperiod.

2.3 | Concurrent Measurements of Gas Exchange and Carbon Isotope Discrimination

Leaf gas exchange and photosynthetic carbon isotope discrimination were measured concurrently using an open-gas exchange system (LI-6800, LI-COR Environmental, Lincoln, NE, USA) incorporating a clear-top controlled environment small leaf chamber (6800-17, LI-COR Environmental, Lincoln, NE, USA) with the small LED light source (6800-02, LI-COR Environmental, Lincoln, NE, USA) enclosing $6\,cm^2$ of leaf (Supporting Information S1: Figure 1A). On enclosure of the leaf, the settings were: chamber inlet $[CO_2]$ at $400\,\mu mol\,mol^{-1}$, initial photosynthetic photon flux density (PPFD) $0\,\mu mol\,m^{-2}\,s^{-1}$, flow rate $350\,\mu mol\,s^{-1}$, air temperature at 25°C, vapour pressure deficit at 1.2 kPa and $[O_2]$ 1.97 kPa (2%). Once respiration was stable, six consecutive measurements were logged manually to measure dark respiration. Next, the auto programme was initiated where PPFD was set to $100\,\mu mol\,m^{-2}\,s^{-1}$ for 24 min before increasing to $1800\,\mu mol\,m^{-2}\,s^{-1}$ for 48 min. Measurements were recorded at 10 s intervals.

The gas-exchange system was coupled to a TDL system (TDL; TGA200a, Campbell Scientific, Inc., Logan, UT, USA) for concurrent measurements of both $[^{12}CO_2]$ and $[^{13}CO_2]$, allowing estimation of $\delta^{13}C$ (Bowling et al. 2003; Evans and Von Caemmerer 2013; Wang et al. 2022). The TDL was connected to the LI-6800 reference air stream using the reference port on the back of the sensor head while the port on the front of the head supplied air from the leaf chamber (Jaikumar et al. 2021). CO_2-free air with 1.97 kPa $[O_2]$ and balance N_2 was produced by mixing two gas streams using precision mass flow controllers (Omega Engineering Inc., Stamford, CT, USA) with a portion of the supply going to the gas exchange system while the remainder was used to calibrate and to correct for drift in the TDL (Jaikumar et al. 2021; Wang et al. 2022; Salesse-Smith et al. 2024).

The TDL was calibrated using the concentration series method, described in detail in Wang et al. (2022). Briefly a 10% CO_2 calibration cylinder was diluted in the N_2/O_2 stream to produce different $[CO_2]$ with the same isotopic composition (Tazoe et al. 2011; Ubierna et al. 2013; Wang et al. 2022). The measurement sequence consisted of eight gas streams: CO_2-free air, followed by three different $[CO_2]$ of the same isotopic signature, air from a calibration tank with a known $[^{12}CO_2]$, $[^{13}CO_2]$ and $\delta^{13}C$ composition (NOAA Global Monitoring Laboratory, Boulder, CO, USA), the IRGA reference and leaf chamber air streams, and the IRGA reference again. As in Wang et al. (2022), each step had a duration of 20 s, except for the leaf chamber air, which had a duration of 600 s with a total cycle time of 740 s. Measurements were collected at 10 Hz and averaged over 10 s into a single data point. The first 10 s of each gas stream was excluded, except for the sample line which produced 59 data points each cycle according to Wang et al. (2022).

Before measurement, plants were kept in the dark overnight, and then transferred to a low PPFD of ca.$10\,\mu mol\,m^{-2}\,s^{-1}$.

Between two and four 8–9-week-old plants of each accession in their vegetative growth phase were used for measurements. The youngest fully expanded trifoliate was selected. Given the vining architecture of the ancestral accessions, the youngest fully expanded trifoliate not overlapped by a neighbouring trifoliate or tendril was chosen. In some cases, the tendril with the selected trifoliate had to be disentangled to reach the leaf chamber (Supporting Information S1: Figure 1B).

2.4 | Calculations of photosynthetic discrimination ($\Delta^{13}C_{obs}$) and mesophyll conductance (g_m)

On-line photosynthetic discrimination ($\Delta^{13}C_{obs}$) was calculated according to Evans et al. 1986:

$$\Delta^{13}C_{obs} = \frac{1000\xi\,(\delta^{13}C_{samp} - \delta^{13}C_{ref})}{1000 + \delta^{13}C_{samp} - \xi(\delta^{13}C_{samp} - \delta^{13}C_{ref})}, \quad (1)$$

where $\delta^{13}C_{samp}$ and $\delta^{13}C_{ref}$ are the carbon isotope compositions of the leaf chamber and reference air in the LI-6800 and ξ is

$$\xi = \frac{C_{ref}}{C_{ref} - C_{samp}}, \quad (2)$$

where C_{ref} and C_{samp} are the CO_2 concentrations of dry air entering and exiting the leaf chamber, respectively, measured by the TDL. A full list of symbols can be found in Table 1.

Mesophyll conductance was estimated according to Evans and Von Caemmerer (2013), accounting for the ternary effect (Farquhar and Cernusak 2012):

$$g_m = \frac{\frac{1+t}{1-t}\left(b - a_i - \frac{eR_d}{(A+R_d)}\right)\frac{A}{C_a}}{\Delta_i - \Delta_o - \Delta_e - \Delta_f}, \quad (3)$$

where b is fractionation associated with Rubisco carboxylation (29‰, Roeske and O'Leary 1984), a_i (1.8‰) denotes the fractionation factor for dissolution and diffusion through water, e denotes the apparent fractionation factor associated with decarboxylation, R_d is the rate of mitochondrial respiration in the light (assumed to be equal to respiration in the dark) and A is the rate of net leaf CO_2 assimilation. Carbon dioxide diffusion from the boundary layer to the sub-stomatal cavity is affected by collisions of the isotopologues of CO_2 with air and with water vapour, a process referred to as the ternary effect. Without accounting for this, conductance would be overestimated. Following Farquhar and Cernusak (2012) the ternary correction factor (t) is obtained as

$$t = \frac{(1 + a')E}{2g^t_{ac}}, \quad (4)$$

where E is the rate of transpiration, g^t_{ac} is the total conductance to CO_2 diffusion in the gas phase including boundary layer and stomatal conductance (von Caemmerer and Farquhar 1981) and

TABLE 1 | Summary abbreviations and their definitions and units.

Variable	Definition	Units	Notes
a_s	Fractionation across the stomata	‰	4.4
a_b	Fractionation across the boundary layer	‰	2.9
a_i	Fractionation factor for dissolution and diffusion through water	‰	1.8
a'	Combined fractionation factor through the leaf boundary layer and stomata	‰	Equation (5)
A	Net CO_2 assimilation rate	$\mu mol\,m^{-2}\,s^{-1}$	
A_c	Rubisco-limited net CO_2 assimilation rate	$\mu mol\,m^{-2}\,s^{-1}$	Equation (15)
A_j	RuBP-regeneration-limited net CO_2 assimilation rate	$\mu mol\,m^{-2}\,s^{-1}$	Equation (16)
$A\vert_{g_{sc}=\infty}$	Modelled assimilation rate expected to occur if stomatal conductance to CO_2 diffusion were infinite	$\mu mol\,m^{-2}\,s^{-1}$	Equation (11)
$A\vert_{g_m=\infty}$	Modelled assimilation rate expected to occur if mesophyll conductance to CO_2 diffusion were infinite	$\mu mol\,m^{-2}\,s^{-1}$	Equation (12)
b	Fractionation associated with Rubisco carboxylation	‰	29 (Roeske and O'Leary 1984)
C_a	Ambient CO_2 partial pressure	$\mu mol\,mol^{-1}$	
C_c	Chloroplastic CO_2 partial pressure/mole fraction	$\mu mol\,mol^{-1}$	
$C_C\vert_{g_{sc}=\infty}$	Value of C_C expected to occur if stomatal conductance to CO_2 diffusion were infinite	$Pa/\mu mol^{-1}$	Equation (13)
$C_C\vert_{g_m=\infty}$	Value of C_C expected to occur if mesophyll conductance to CO_2 diffusion were infinite	$Pa/\mu mol^{-1}$	Equation (14)
C_i	Intercellular CO_2 partial pressure/mole fraction	$\mu mol\,mol^{-1}$	
C_s	CO_2 partial pressure at the leaf surface	$\mu mol\,mol^{-1}$	
e	Respiratory fractionation during decarboxylation (respiratory fractionation)	‰	0 (Ubierna et al. 2013)
e'	Fractionation during decarboxylation including measurement artefacts	‰	Equation (6)
E	Transpiration rate	$mol\,H_2O\,m^{-2}\,s^{-1}$	
f	Fractionation during photorespiration	‰	11.6 in this study
g_m	Mesophyll conductance	$\mu mol\,m^{-2}\,s^{-1}\,Pa$ or bar^{-1}	Equation (3)
g_{sc}	Stomatal conductance to CO_2 diffusion; $g_{sc} = g_{sw}/1.6$	$mol\,m^{-2}\,s^{-1}$	
g_{sw}	Stomatal conductance to water vapour	$mol\,m^{-2}\,s^{-1}$	
g_{ac}^t	Total conductance to CO_2 diffusion between boundary layer and stomatal conductance	$mol\,total\,m^{-2}\,s^{-1}$	
J	Light-dependent RuBP regeneration rate	$\mu mol\,m^{-2}\,s^{-1}$	Equation (18)
l_s^{Warren}	Relative limiting factor due to stomatal conductance in the Warren et al. (2003) framework	%	Equation (11)
l_m^{Warren}	Relative limiting factor due to mesophyll conductance in the Warren et al. (2003) framework	%	Equation (12)
O	O_2 partial pressure	Pa	
PPFD	Photosynthetic Photon Flux Density	$\mu mol\,m^{-2}\,s^{-1}$	
R_d	Mitochondrial respiration in the light	$\mu mol\,CO_2\,m^{-2}\,s^{-1}$	
$S_{c/o}$	Rubisco specificity factor	$mol\,CO_2/mol\,O_2$	
t	Ternary effect	‰	Equation (4)

(Continues)

TABLE 1 | (Continued)

Variable	Definition	Units	Notes
t_{50g_m}	time taken for mesophyll conductance to reach 50% of its steady-state value	minutes	
t_{90g_m}	time taken for mesophyll conductance to reach 90% of its steady-state value	minutes	
V_{cmax}	Maximum Rubisco carboxylation rate	$\mu mol\,m^{-2}\,s^{-1}$	Equation (17)
WUEi	Intrinsic water-use efficiency	$mol\,CO_2\,mol^{-1}\,H_2O$	A/g_{sw}
$\Delta^{13}C_{obs}$	Photosynthetic discrimination	‰	Equation (1)
Δ_e	Fraction associated with respiration	‰	Equation (8)
Δ_f	Fractionation associated with photorespiration	‰	Equation (9)
Δ_i	Fractionation if $C_i = C_c$ in the absence of any respiratory fraction	‰	Equation (7)
Γ^*	CO_2 compensation point in the absence of mitochondrial respiration in the light	Pa or bar	Equation (10)
ξ	Ratio of $^{12}CO_2$ mole fraction in the dry air coming into the gas-exchange cuvette over the difference in $^{12}CO_2$ mole fractions of air in and out of the cuvette	unitless	Equation (2)

TABLE 2 | Summary of soybean accession information.

Species	Accession	Maturity group	Country of origin
Glycine soja Siebold & Zucc	Anc297 (*PI 407297*)[a]	II	Liaoning Sheng, China
	Anc460 A (*PI 483460 A*)[a]	III	Liaoning Sheng, China
	Anc460 B (*PI 483460 B*)[a]	III	Liaoning Sheng, China
	Anc399 B (*PI 468399 B*)[a]	IV	Shandong Sheng, China
Glycine max (L.) Merr	LD11 (LD11-2170)[b]	III	Illinois, United States

[a]U.S. National Plant Germplasm System (https://npgsweb.ars-grin.gov/gringlobal/search).
[b]Cai and Brock (2021).

a' denotes the combined fractionation factor through the leaf boundary layer and stomata:

$$a' = \frac{a_b(C_a - C_s) + a_s(C_s - C_i)}{C_a - C_i}, \qquad (5)$$

where C_a, C_s and C_i are the ambient, leaf surface and intercellular CO_2 partial pressures, a_b (2.9‰) is the fractionation occurring through diffusion in the boundary layer and a_s (4.4‰) is the fractionation due to diffusion in the air (Evans et al. 1986).

The apparent fractionation during decarboxylation includes two terms, such that $e = e' + e_0$. The first term e' represents the influence of measurement artifacts, defined as

$$e' = \delta^{13}C_{ref} - \delta^{13}C_{gatm} \qquad (6)$$

while e_0 is the respiratory fractionation during decarboxylation, taken to be 0‰ in this study (Evans and Von Caemmerer 2013; Ubierna et al. 2013). $\delta^{13}C_{ref}$ is the isotopic signature of the CO_2 entering the LI-6800 reference and $\delta^{13}C_{gatm}$ (−8‰) is the isotopic compositions of the CO_2 where the plants are grown. Δ_i is the discriminations that would occur if $C_i = C_c$ in the absence of any respiratory fractionation ($e = 0$):

$$\Delta_i = \frac{1}{(1-t)}a' + \frac{1}{(1-t)}((1+t)b - a')\frac{C_i}{C_a} \qquad (7)$$

Δ_e is the fractionation associated with respiration:

$$\Delta_e = \frac{1+t}{1-t}\left(\frac{eR_d}{(A+R_d)C_a}(C_i - \Gamma^*)\right), \qquad (8)$$

Δ_f is the fractionation associated with photorespiration:

$$\Delta_f = \frac{1+t}{1-t}\left(f\frac{\Gamma^*}{C_a}\right), \qquad (9)$$

where f is the photorespiratory fractionation factor assumed to be 11.2‰ (Lanigan et al. 2008) and Δ_f is linearly related to O_2 concentration via the CO_2 compensation point in the absence of respiration (Γ^*):

$$\Gamma^* = \frac{O}{2S_{c/o}}, \qquad (10)$$

where O is the $[O_2]$ partial pressure and $S_{c/o}$ is the Rubisco specificity factor (von Caemmerer, 2000).

2.5 | Calculations of Limiting Factors

Dimensionless factors representing the limitations placed on the photosynthetic CO_2 assimilation rate by CO_2 diffusion or biochemistry were calculated using two different frameworks (Warren et al. 2003; Grassi and Magnani 2005) using the *calculate_c3_limitations_warren* and *calculate_c3_limitations_grassi* functions from the *PhotoGEA* R package (Lochocki 2024). Here, we describe the Warren et al. (2003) framework, the Grassi and Magnani (2005) framework can be found in Supporting Information S1: Methods.

Limiting factors during induction were calculated using the 4-min averages of A, g_{sw}, g_m, C_i and C_c, as described in detail below. The Warren et al. (2003) framework defines limiting factors due to stomatal and mesophyll conductance, which we refer to here as l_s^{Warren} and l_m^{Warren}:

$$l_s^{\text{Warren}} = \frac{A|_{g_{sc}=\infty} - A_n}{A|_{g_{sc}=\infty}}, \quad (11)$$

$$l_m^{\text{Warren}} = \frac{A|_{g_m=\infty} - A_n}{A|_{g_m=\infty}}, \quad (12)$$

where A is the measured assimilation rate and $A|_{g_{sc}=\infty}$ and $A|_{g_m=\infty}$ are modelled assimilation rates expected to occur if g_{sc} (stomatal conductance to CO_2 diffusion $g_{sc} = g_{sw}/1.6$) or g_m were infinite, respectively. These modelled rates can be calculated by first defining corresponding values of C_c using $C_c = C_a - \Delta C_s - \Delta C_m$, where $\Delta C_s = C_a - C_i$ and $\Delta C_m = C_i - C_c$ are the [CO_2] drawdowns across the stomata and mesophyll, respectively, and C_a, C_i and C_c are the measured ambient, intercellular and chloroplast [CO_2], respectively. If conductance across a barrier (stomata or mesophyll) is infinite, the drawdown across it is zero:

$$C_C|_{g_{sc}=\infty} = C_a - 0 - (C_i - C_c) = C_a - C_i + C_c, \quad (13)$$

$$C_C|_{g_m=\infty} = C_a - (C_a - C_i) - 0 = C_i, \quad (14)$$

where $C_C|_{g_{sc}=\infty}$ and $C_C|_{g_m=\infty}$ are chloroplast [CO_2] that expected to occur if g_{sc} or g_m were infinite, respectively. With these, it is possible to calculate the modelled assimilation rates using the Farquhar-von-Caemmerer-Berry model (von Caemmerer, 2000) under two scenarios, where assimilation is either Rubisco-limited A_c or RuBP-regeneration-limited A_j:

$$A_c = \frac{V_{c\max} \cdot (C_c - \Gamma^*)}{C_c + K_M} - R_d, \quad (15)$$

$$A_j = \frac{J \cdot (C_c - \Gamma^*)}{4 \cdot C_c + 8 \cdot \Gamma^*} - R_d, \quad (16)$$

where $V_{c\max}$ is the maximum Rubisco carboxylation rate, J is the light-dependent whole chain electron transport rate, $K_M = K_c \cdot (1 + O/K_o)$ is the effective Michaelis–Menten constant for Rubisco carboxylation, K_c and K_o are the Michaelis–Menten constants for [CO_2] and [O_2], and O is the oxygen concentration in the chloroplast (assumed to be 1.97 kPa, equal to the ambient value in the leaf chamber). Values of K_c and K_o were calculated from the leaf temperature as described previously (Bernacchi et al. 2001).

Both frameworks require values of $V_{c\max}$ and J, which can be estimated from the measured values of A_n, C_c, and R_d by assuming either Rubisco-limited or RuBP-regeneration-limited assimilation and solving Equations (15) and (16) for $V_{c\max}$ and J, respectively:

$$V_{c\max} = \frac{(A_n + R_d) \cdot (C_c + K_M)}{C_c - \Gamma^*}, \quad (17)$$

$$J = \frac{(A_n + R_d) \cdot (4 \cdot C_c + 8 \cdot \Gamma^*)}{C_c - \Gamma^*}. \quad (18)$$

The induction curves measured here do not provide enough information to determine whether assimilation is limited by Rubisco or RuBP regeneration, so each set of limiting factors was calculated under each scenario. However, prior work with soybean cultivars have suggested Rubisco and not RubP regeneration is the predominant biochemical limitation throughout induction (Soleh et al. 2016, 2017; Taylor and Long 2017). Note, that as written, Equations (11) and (12) calculate dimensionless limiting factors, which are multiplied by 100 to express them as percentages.

2.6 | Data Processing and Statistical Analysis

An automatic data processing and g_m calculation tool was developed in MATLAB (v2019a, Mathworks, https://uk.mathworks.com). MATLAB used the pretreated gas exchange data files (csv file with parameters needed for calculation) and the raw TDL data files to calculate the g_m through the photosynthetic induction, with the equations described earlier. The data that support the findings of this study are available at: https://doi.org/10.13012/B2IDB-7809185_V2.

Unreasonable values of g_m ($g_m \geq 1$ or $g_m \leq 0$ and those associated with $\xi \geq 50$ or $\xi \leq 0$) were removed before analysis. Data points were grouped into 4-min intervals and the interquartile range was calculated to remove outliers within each interval before averaging. Due to noise within each replicate, the moving average of g_m was then calculated. Values of A, C_i, C_c, g_{sw} and WUEi were also grouped and averaged into 4-min intervals. Only the response of photosynthetic parameters after the increase in PPFD from 100 to 1800 was evaluated; therefore, values of light induction and steady state were calculated as the average of the initial and last 12 min (three 4-min intervals) after the increase in light intensity. Statistical analyses ($p < 0.1$ significance level) were performed using repeated measures ANOVA where accession and time were main effects. The residuals were checked for normality and constant variance, box Cox transformations were conducted if these criteria were unmet. Means comparison Dunnett test using LD11 as the control was performed if there was a significant accession effect and/or significant interaction between accession and time (R software, R Core Team 2021). Curve fitting (3 parameter Sigmoidal Hill) was conducted in SigmaPlot (SigmaPlot 15, Systat

Software) for the calculation of the time taken for g_m to reach 50% (t_{50g_m}) and 90% (t_{90g_m}) of its steady-state value where a one-way ANOVA was conducted for statistical analysis (Supporting Information S1: Figures 2–6).

3 | Results

3.1 | The Response of Mesophyll Conductance (g_m) and Other Photosynthetic Parameters after an Increase in Light Intensity

Steady-state g_m was significantly greater (ca. 70%) in the elite modern cultivar (LD11) than the average of the four ancestors (Figure 1A,B and Supporting Information S1: Table S1). Despite attaining this higher g_m, induction in LD11 was as rapid as in the ancestors (Figure 1C and Supporting Information S1: Figures 2-6). Steady-state net leaf CO_2 assimilation rate (A) of LD11 was significantly higher and almost twice that of the ancestral accessions, as was the average A over the first 12 min of induction following transfer from low to high light (Figure 2). At steady state and throughout induction intercellular and stromal [CO_2] (C_i and C_c, respectively) were substantially lower in the modern elite (LD11) (Figure 3). C_i and C_c briefly decreased after the increase in light intensity before reaching a plateau, which was close to the shade value for the ancestral accessions, but below that for LD11 (Figure 3). In contrast to g_m, stomatal conductance (g_{sw}) was not significantly higher than the ancestral accessions, both at steady state and through induction (Figure 4). Coincided with this and the higher A of the elite is a higher leaf instantaneous water use efficiency (Figure 4).

3.2 | The Limitation on Net CO_2 Assimilation Rate (A)

The dynamics of the two gas diffusional limiting factors (g_m and g_{sw}) affecting A under the assumption of RuBP regeneration (J) and Rubisco carboxylation (V_{cmax}) biochemical limitation were evaluated using the methods described in Warren et al. (2003). Since g_m and A of LD11 were found to be significantly higher than for all four ancestral accessions, the limitation comparisons were made between species where the response of all four
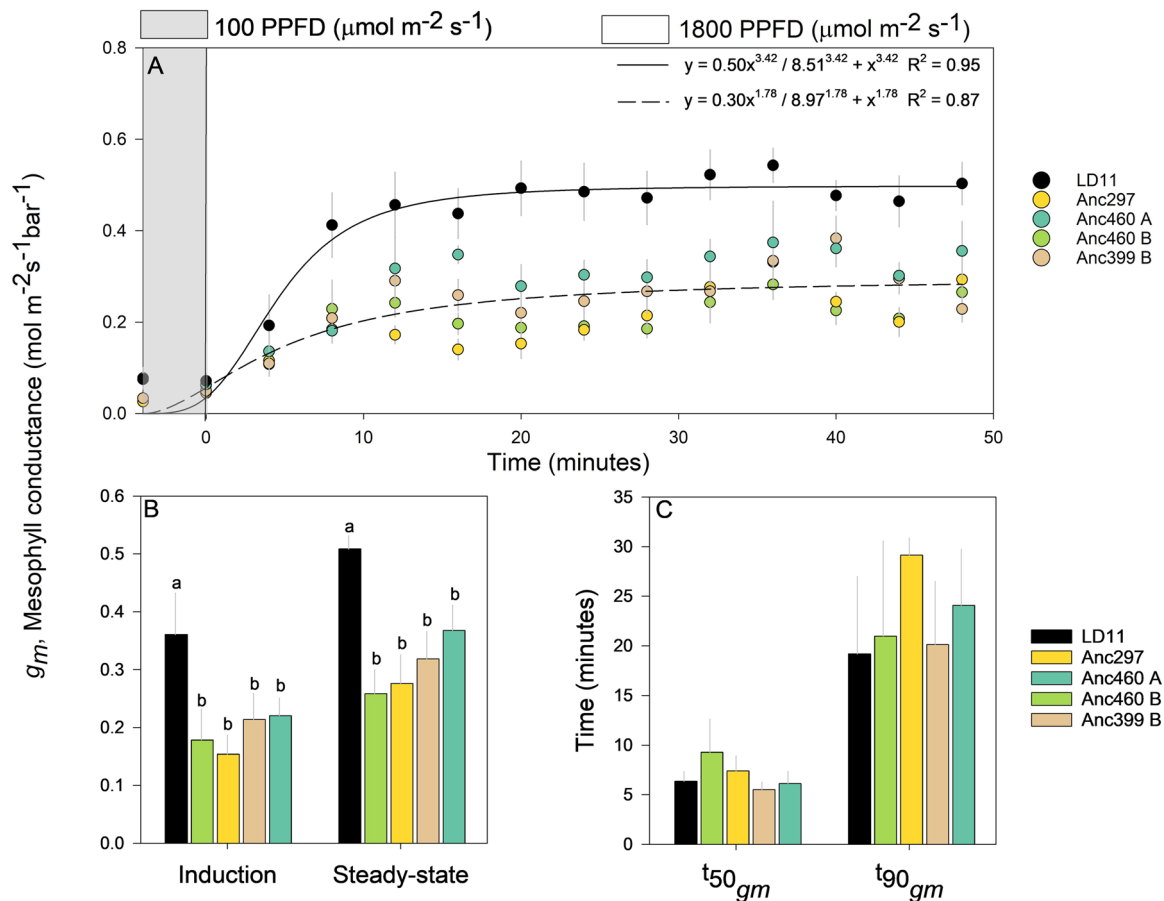
FIGURE 1 | Comparisons among domesticated high-yielding elite LD11 (*Glycine max* (L.) Merr) and four ancestor accessions (*Glycine soja* Siebold & Zucc) illustrated as (A) the average temporal response of mesophyll conductance (g_m) after a transition in photosynthetic photon flux density (PPFD) from 100 (grey area) to 1800 (white area) where data points represent 4-min moving averages, solid black line and dashed black line represent the fitted sigmoidal Hill regression of the elite and ancestors, respectively, (B) the average response of g_m during light induction and at steady state, and (C) the time taken for g_m to reach 50% (t_{50g_m}) and 90% (t_{90g_m}) of its steady-state value. Light induction and steady state were defined as the initial and last 12 min (three 4-min intervals) after an increase in light intensity, respectively. Different letters indicate significant differences ($p < 0.1$, repeated measures ANOVA, $n = 12$) and error bars indicate standard error.
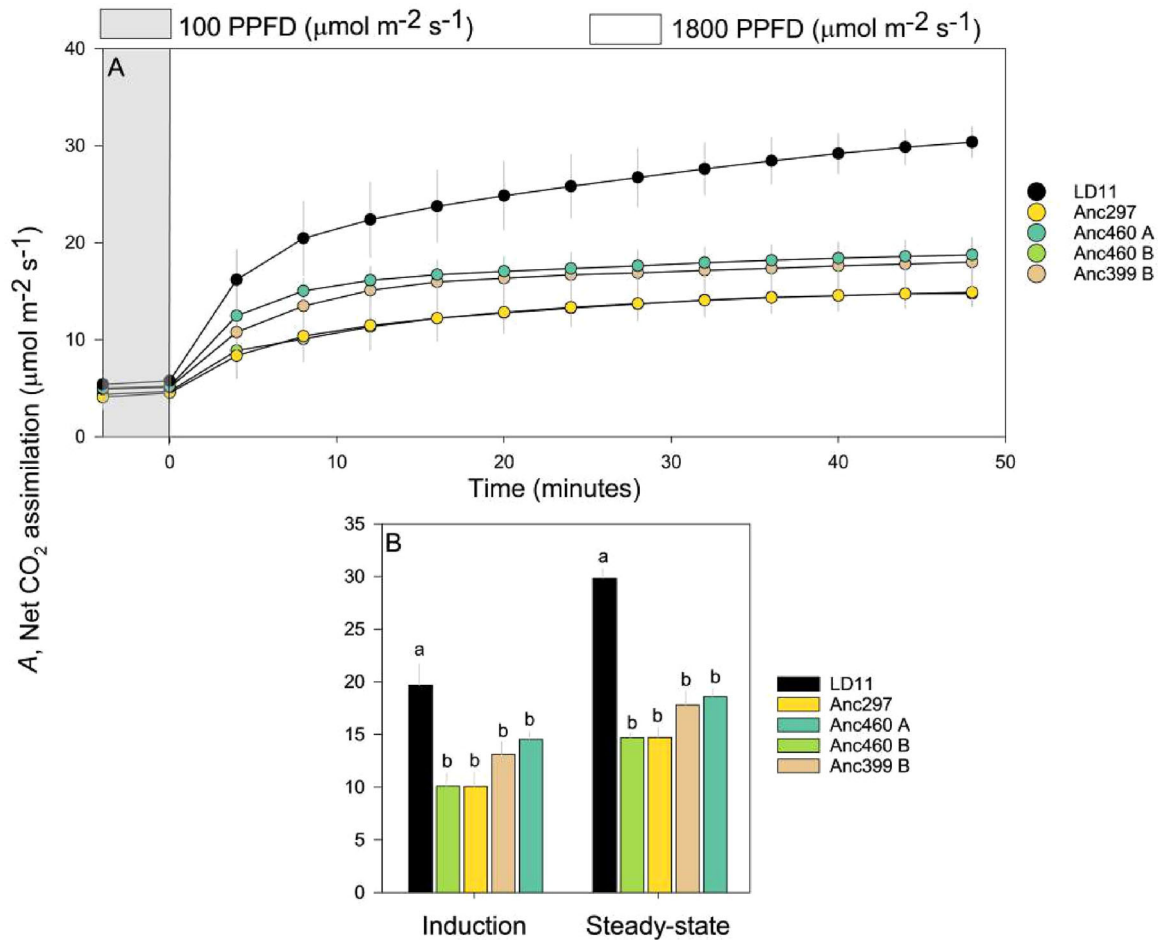
FIGURE 2 | Comparisons among domesticated high-yielding elite LD11 (*Glycine max* (L.) Merr) and four ancestor accessions (*Glycine soja* Siebold & Zucc) illustrated as (A) the average temporal response of net CO_2 assimilation (A) after a transition in photosynthetic photon flux density (PPFD) from 100 (grey area) to 1800 (white area) where data points represent 4-min averages, (B) the average response of A during light induction and at steady state. Light induction and steady state were defined as the initial and last 12 min (three 4-min intervals) after an increase in light intensity, respectively. Different letters indicate significant differences ($p < 0.1$, repeated measures ANOVA, $n = 12$) and error bars indicate standard error. [Color figure can be viewed at wileyonlinelibrary.com]

ancestral accessions was represented by a combined average (*G. max* and *G. soja*, respectively).

Limitations analysis showed that regardless of whether RubP regeneration or Rubisco carboxylation was assumed as the biochemical limitation, the limitations on A imposed by both stomatal and mesophyll conductance were greater in the elite modern soybean at steady state and through induction (Figure 5). The limitations on A by both g_m and g_{sw} followed similar trends but were more severe under carboxylation than regeneration biochemical limitation through induction and at steady state (Figure 5). The limitation of g_{sw} was also greater than g_m under both biochemical limitation assumptions (Figure 5C,D). Limitations calculated using the methods described in Grassi and Magnani (2005), although different in scale, compare well to the conclusions from the Warren et al. (2003) method (Supporting Information S1: Figures 7AB and 8AB). The Grassi and Magnani (2005) framework also calculates biochemical limitations in addition to diffusion limitations; limitations imposed by J or V_{cmax} on A were higher for *G. soja* than *G. max* during both the induction and steady-state phases (Supporting Information S1: Figures 7C and 8C).

4 | Discussion

This study tested two hypotheses concerning the domestication and subsequent improvement of soybean, both are strongly supported by the results obtained. (1) Mesophyll conductance (g_m) was shown to be a significant limitation to soybean photosynthesis both at steady state and through light induction especially when the major biochemical limitation was in vivo Rubisco activity (V_{cmax}) (Figure 5). (2) Compared to the ancestral accessions, the elite soybean cultivar showed a near doubling and significant increase in g_m at both steady state and through light induction (Figure 1), which also corresponded to a substantial increase in leaf CO_2 assimilation (A) and leaf level water use efficiency (WUEi, Figures 2 and 4). It also shows that domestication and breeder selection for yield had resulted in a large increase in leaf photosynthetic rate (Figure 2).

Further examination investigating the g_m response to light induction across a broader range of ancestral accessions as well as different domesticated accessions of soybean by year of release may strengthen the conclusions here. Previous research has explored historical soybean accessions between 1923 and 2007
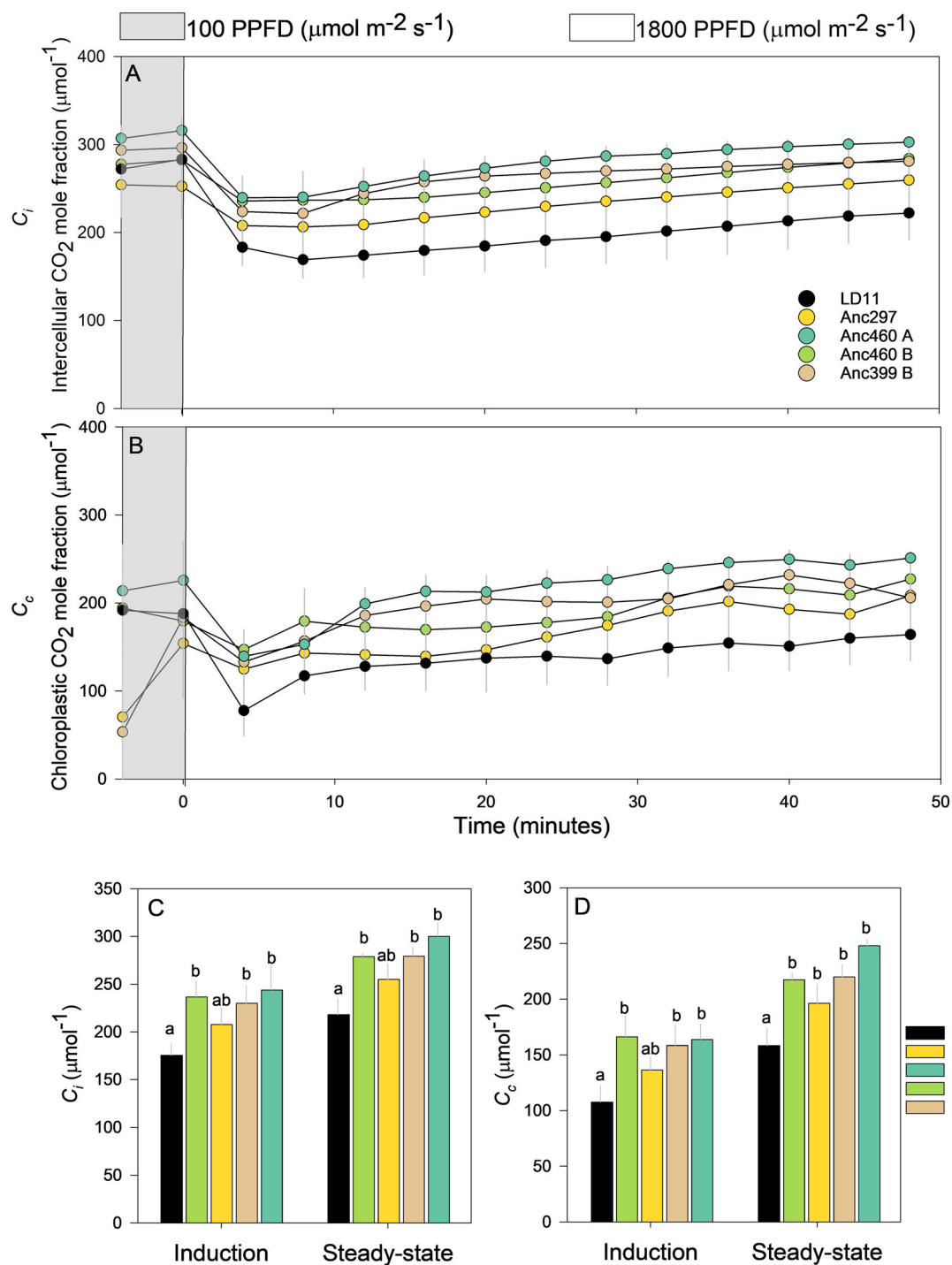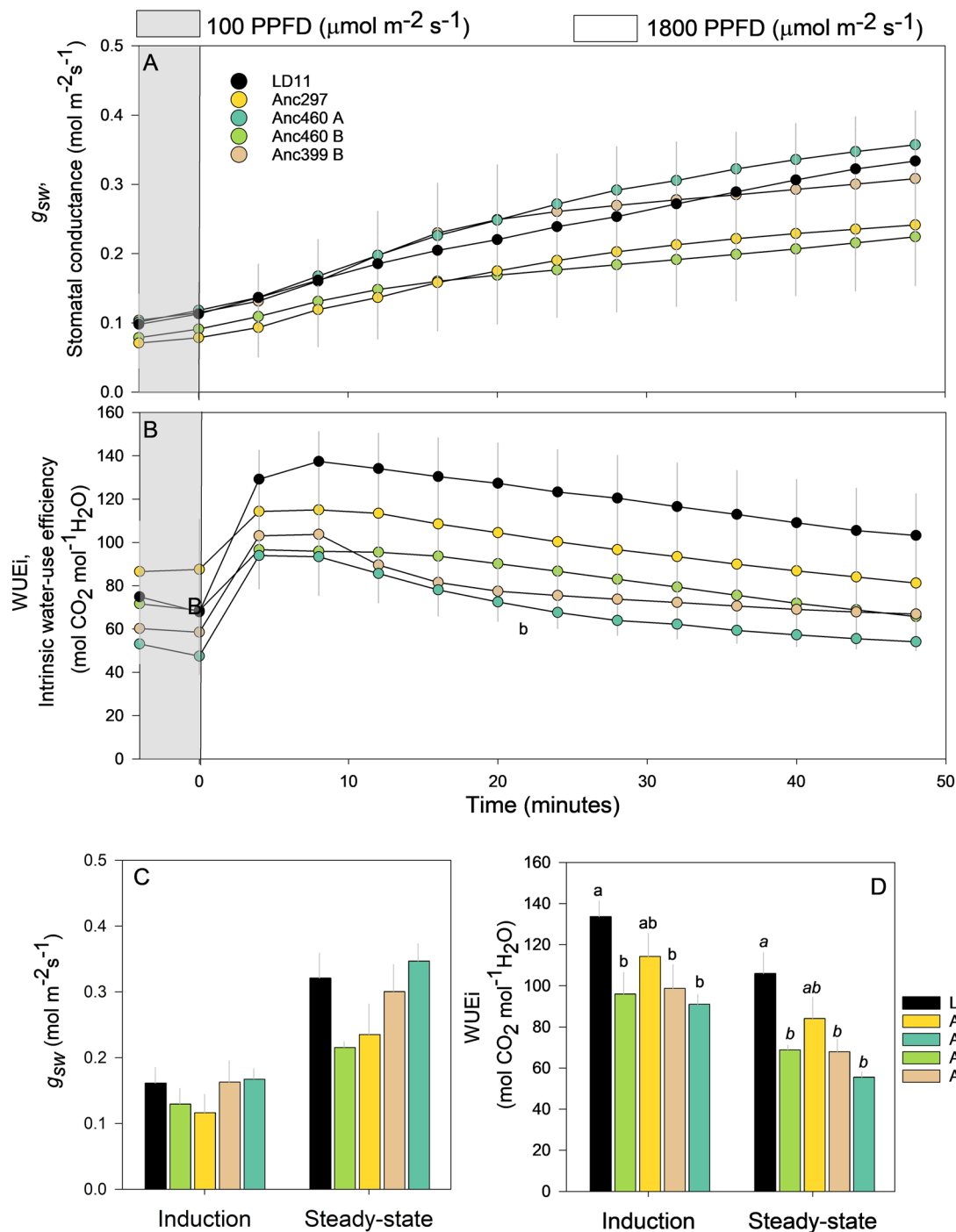
FIGURE 3 | Comparisons among domesticated high-yielding elite LD11 (*Glycine max* (L.) Merr) and four ancestor accessions (*Glycine soja* Siebold & Zucc) illustrated as the average temporal response of (A) intercellular CO_2 mole fraction (C_i) and (B) chloroplastic CO_2 mole fraction (C_c) after a transition in photosynthetic photon flux density (PPFD) from 100 (grey area) to 1800 (white area) where data points represent 4-min averages, the average response of (C) C_i and (D) C_c during light induction and at steady state. Light induction and steady state were defined as the initial and last 12 min (three 4-min intervals) after an increase in light intensity, respectively. Different letters indicate significant differences ($p < 0.1$, repeated measures ANOVA, $n = 12$) and error bars indicate standard error. [Color figure can be viewed at wileyonlinelibrary.com]

where steady-state A/C_i responses using the Variable J method revealed that g_m has not changed consistently with release date (Koester et al. 2016). Evaluation under dynamic light conditions with the isotopic discrimination technique may challenge these conclusions. We acknowledge that the equations used here to calculate g_m (Evans and Von Caemmerer 2013) are not the most recent. Busch et al. (2020) modified the assumptions related to the mitochondrial respiration fractionation component which improved the accuracy of g_m when intercellular $[CO_2]$ (C_i) values are low ($< 100 \mu mol\ mol^{-1}$). Here, C_i did not drop below 150 μmol mol^{-1} during light induction (Figure 3A) and Supporting Information S1: Figure 9 shows negligible differences between g_m
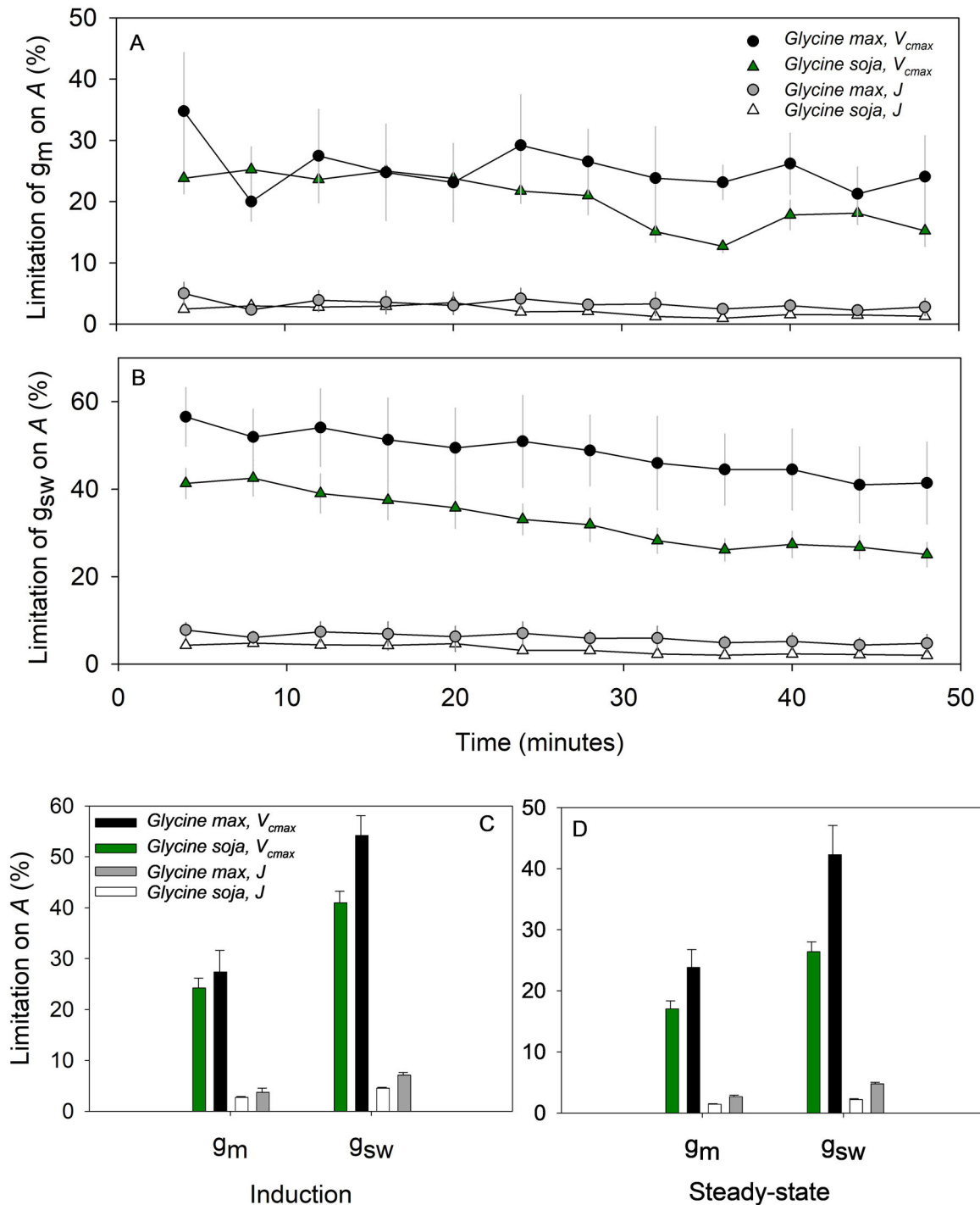
FIGURE 4 | Comparisons among domesticated high-yielding elite LD11 (*Glycine max* (L.) Merr) and four ancestor accessions (*Glycine soja* Siebold & Zucc) illustrated as the average temporal response of (A) stomatal conductance (g_{sw}) and (B) intrinsic water-use efficiency (WUEi) after a transition in photosynthetic photon flux density (PPFD) from 100 (grey area) to 1800 (white area) where data points represent 4-min averages, the average response of (C) g_{sw} and (D) WUEi during light induction and at steady state. Light induction and steady state were defined as the initial and last 12 min (three 4-min intervals) after an increase in light intensity, respectively. Different letters indicate significant differences ($p < 0.1$, repeated measures ANOVA, $n = 12$, where italic letters indicate $p = 0.12$) and error bars indicate standard error. [Color figure can be viewed at wileyonlinelibrary.com]

calculated of Busch et al. (2020) relative to Evans and Von Caemmerer (2013) under the measurement conditions used in this study. More replicate power may also reduce the noise associated with the speed of g_m response to light induction (Figure 1C and Supporting Information S1: Figures 2–6). Nonetheless, such techniques require proficiency and specialized

equipment where labour and costs may need to be compromised in screening large amounts of germplasm.

Mesophyll conductance is a suggested target for improvement, since it would result in higher rates of CO_2 assimilation per unit leaf area, without any increased cost in terms of water use, so

FIGURE 5 | The limitation of mesophyll conductance (g_m) and stomatal conductance (g_{sw}) on net CO_2 assimilation rate (A) after an increase in light intensity over time (A, B), and the average limitation during light induction (C) and steady state (D) assuming the biochemical limitations of ribulose 1,5-biphosphosphate (RuBP) carboxylation (V_{cmax}) and regeneration (J). Limitation calculations were made using the methods described in Warren et al. (2003). The comparisons are between domesticated high-yielding elite LD11 (*Glycine max* (L.) Merr, $n = 4$) and the average of four ancestor accessions (*Glycine soja* Siebold & Zucc, $n = 16$). Light induction and steady state were defined as the initial and last 12 min (three 4-min intervals) after an increase in light intensity, respectively. Error bars indicate standard error. [Color figure can be viewed at wileyonlinelibrary.com]

potentially providing a sustainable increase in crop productivity (Flexas et al. 2013; Lundgren and Fleming 2020; Long et al. 2022; Salesse-Smith et al. 2024). Here, it was shown to be a substantial limitation to light-saturated A at steady state (ca. 20%) and more so in the elite LD11 than the ancestral accessions when $V_{c,max}$ was the major biochemical limitation

(Figure 5). Most previous studies have estimated g_m under steady-state conditions. However, the light environment in dense modern crop canopies is rarely constant, with most leaves experiencing many fluctuations in light over the course of a day (Long et al. 2022). On transition of leaves from shade to sun, g_{sw} and g_m increase over several minutes, and contribute to the

slow increase in A. Under these conditions the limitation attributable to g_m (ca. 25%) was even greater than at steady state, showing the importance of considering light fluctuation for field crops. The limitation, at both steady state and through induction, was only slight when regeneration of RuBP, governed by the maximum rate of whole chain electron transport (J), is assumed the biochemical limitation (Figure 5). However, previous analyses of A/C_i responses of a range of soybean germplasm showed that in the current atmosphere, $V_{c,max}$ and not J_{max} as the exclusive biochemical limitation at both light-saturated steady-state A and through light-induction (Sakoda et al. 2016; Soleh et al. 2016, 2017). The results therefore suggest a strong limitation on assimilation by g_m; a limitation which has decreased through selection in domestication and subsequent breeding.

As a major limitation to assimilation under current and past atmospheric [CO_2], it might be expected that domestication and breeding would have indirectly selected for increased g_m, particularly for the most recent soybean releases, which appear strongly source limited (Ainsworth and Long, 2021). The ca. 70% increase in g_m in LD11 compared to the ancestral accessions, corresponds to a near doubling of light-saturated A (Figures 1 and 2) implying that g_m has scaled with increase in A. However, while increased g_m and the associated increased WUEi may have indirectly resulted from selection of more productive accessions, it appears that g_m has not kept pace with increased A. Despite higher g_m in the elite cultivar, C_i was ca. 60 μmol mol^{-1} lower at light-saturated steady state (Figure 3) which would substantially increase photorespiration and decrease the rate of carboxylation. This finding implies that improvement of g_m has been less than the increase in biochemical capacity for CO_2 assimilation, and suggests g_m is an important target for improving both productivity and water use efficiency in soybean.

Manipulation of cell wall porosity has been suggested as one means to substantially increase g_m (Evans 2021). In tobacco, transgenic upregulation of a pectin methyltransferase increased cell wall porosity, with concomitant significantly increased g_m and A, suggest one way to achieve this in soybean (Salesse-Smith et al. 2024). However, the large differences in g_m found here between the wild ancestors and an elite line suggest that there may be substantial variation within soybean germplasm that might be exploited through marker-assisted breeding, genomic selection, or direct selection through measurement of g_m. Substantial variation in g_m and associated improvement in WUE has been shown in other crops (Barbour et al. 2010; Jahan et al. 2014; Tomás et al. 2014). In soybean, a survey of 12 cultivars showed a two-fold variation in g_m. This was strongly and positively correlated with variation in A, where 38% of the variation was due to cultivar (Tomeo and Rosenthal 2017). These results suggest g_m has unexplored potential within soybean breeding to deliver increased productivity and water use efficiency.

Acknowledgements

Data Availability Statement

The data that support the findings of this study are openly available in Soybean/Soja mesophyll conductance during light induction at https://doi.org/10.13012/B2IDB-7809185_V2.

References

Acevedo-Siaca, L. G., R. Coe, Y. Wang, J. Kromdijk, W. P. Quick, and S. P. Long. 2020. "Variation in Photosynthetic Induction Between Rice Accessions and Its Potential for Improving Productivity." *New Phytologist* 227: 1097–1108.

Adeniyan, O. N., and O. T. Ayoola. 2006. "Growth and Yield Performance of Some Improved Soybean Varieties as Influenced by Intercropping with Maize and Cassava in Two Contrasting Locations in Southwest Nigeria." *African Journal of Biotechnology* 5: 1886–1889.

Ainsworth, E. A., and S. P. Long. 2021. "30 Years of Free-Air Carbon Dioxide Enrichment (FACE): What Have We Learned about Future Crop Productivity and Its Potential for Adaptation?" *Global Change Biology* 27: 27–49.

Anderson, E. J., M. L. Ali, W. D. Beavis, et al. 2019. "Soybean *Glycine max* (L.) Merr. Breeding: History, Improvement, Production and Future Opportunities." *Advances in Plant Breeding Strategies: Legumes* 7: 431–516.

Barbour, M. M., C. R. Warren, G. D. Farquhar, G. Forrester, and H. Brown. 2010. "Variability in Mesophyll Conductance Between Barley Genotypes, and Effects on Transpiration Efficiency and Carbon Isotope Discrimination." *Plant Cell Environment* 33: 1176–1185.

Bernacchi, C. J., A. R. Portis, H. Nakano, S. von Caemmerer, and S. P. Long. 2002. "Temperature Response of Mesophyll Conductance. Implications for the Determination of Rubisco Enzyme Kinetics and for Limitations to Photosynthesis in Vivo." *Plant Physiology* 130: 1992–1998.

Bernacchi, C. J., E. L. Singsaas, C. Pimentel, A. R. Portis, Jr., and S. P. Long. 2001. "Improved Temperature Response Functions for Models of Rubisco-Limited Photosynthesis." *Plant, Cell & Environment* 24: 253–259.

Bowling, D. R., S. D. Sargent, B. D. Tanner, and J. R. Ehleringer. 2003. "Tunable Diode Laser Absorption Spectroscopy for Stable Isotope Studies of Ecosystem-Atmosphere CO_2 Exchange." *Agricultural and Forest Meteorology* 118: 1–19.

Burgess, A. J., C. Masclaux-Daubresse, G. Strittmatter, et al. 2023. "Improving Crop Yield Potential: Underlying Biological Processes and Future Prospects." *Food and Energy Security* 12: e435.

Busch, F. A., M. Holloway-Phillips, H. Stuart-Williams, and G. D. Farquhar. 2020. "Revisiting Carbon Isotope Discrimination in C$_3$

Plants Shows Respiration Rules When Photosynthesis Is Low." *Nature Plants* 6: 245–258.

von Caemmerer, S. 2000. *Biochemical Models of Leaf Photosynthesis*. Clayton, VIC: CSIRO Publishing.

von Caemmerer, S., and J. R. Evans. 2015. "Temperature Responses of Mesophyll Conductance Differ Greatly between Species." *Plant, Cell & Environment* 38: 629–637.

von Caemmerer, S., and G. D. Farquhar. 1981. "Some Relationships between the Biochemistry of Photosynthesis and the Gas Exchange of Leaves." *Planta* 153: 376–387.

Cai, G., and A. Brock 2021. "*The Uniform Soybean Tests: Northern Regions 2021*, 404." West Lafayette, IN: USDA-ARS.

Dermody, O., S. P. Long, and E. H. DeLucia. 2006. "How Does Elevated CO_2 or Ozone Affect the Leaf-Area Index of Soybean When Applied Independently." *New Phytologist* 169: 145–155.

Evans, J. R. 2021. "Mesophyll Conductance: Walls, Membranes and Spatial Complexity." *New Phytologist* 229: 1864–1876.

Evans, J. R., and S. Von Caemmerer. 2013. "Temperature Response of Carbon Isotope Discrimination and Mesophyll Conductance in Tobacco." *Plant, Cell & Environment* 36: 745–756.

Evans, J. R., T. D. Sharkey, J. A. Berry, and G. D. Farquhar. 1986. "Carbon Isotope Discrimination Measured Concurrently with Gas-Exchange to Investigate CO_2 Diffusion in Leaves of Higher Plants." *Australian Journal of Plant Physiology* 13: 281–292.

Farquhar, G. D., and L. A. Cernusak. 2012. "Ternary Effects on the Exchange of Isotopologues of Carbon Dioxide." *Plant, Cell & Environment* 35: 1221–1231.

Flexas, J., M. Carriquí, and F. J. Cano, et al. 2018. "CO2 Diffusion Inside Photosynthetic Organs." In *Leaf: A Platform for Performing Photosynthesis*, edited by W. W. AdamsI and I. Terashima, 163–208. Springer International Publishing AG.

Flexas, J., Ü. Niinemets, A. Gallé, et al. 2013. "Diffusional Conductances to CO_2 as a Target for Increasing Photosynthesis and Photosynthetic Water-Use Efficiency." *Photosynthesis Research* 117: 45–59.

Flexas, J., M. Ribas-carbó, A. Diaz-espejo, J. Galmés, and H. Medrano. 2008. "Mesophyll Conductance to CO_2: Current Knowledge and Future Prospects." *Plant, Cell & Environment* 31: 602–621.

Grassi, G., and F. Magnani. 2005. "Stomatal, Mesophyll Conductance and Biochemical Limitations to Photosynthesis as Affected by Drought and Leaf Ontogeny in Ash and Oak Trees." *Plant, Cell & Environment* 28: 834–849.

Harley, P. C., F. Loreto, G. Dimarco, and T. D. Sharkey. 1992. "Theoretical Considerations When Estimating the Mesophyll Conductance to CO_2 Flux by Analysis of the Response of Photosynthesis to CO_2." *Plant Physiology* 98: 1429–1436.

Jahan, E., J. S. Amthor, G. D. Farquhar, R. Trethowan, and M. M. Barbour. 2014. "Variation in Mesophyll Conductance Among Australian Wheat Genotypes." *Functional Plant Biology* 41: 568–580.

Jaikumar, N. S., S. S. Stutz, S. B. Fernandes, et al. 2021. "Can Improved Canopy Light Transmission Ameliorate Loss of Photosynthetic Efficiency in the Shade? An Investigation of Natural Variation in *Sorghum bicolor*." *Journal of Experimental Botany* 72: 4965–4980.

Kaiser, E., J. Kromdijk, J. Harbinson, E. Heuvelink, and L. F. M. Marcelis. 2017. "Photosynthetic Induction and Its Diffusional, Carboxylation and Electron Transport Processes as Affected by CO_2 Partial Pressure, Temperature, Air Humidity and Blue Irradiance." *Annals of Botany* 119: 191–205.

Kamara, A. Y., A. I. Tofa, T. Ademulegun, et al. 2019. "Maize-Soybean Intercropping for Sustainable Intensification of Cereal-Legume Cropping Systems in Northern Nigeria." *Experimental Agriculture* 55: 73–87.

Kim, M. Y., K. Van, Y. J. Kang, K. H. Kim, and S.-H. Lee. 2012. "Tracing Soybean Domestication History: From Nucleotide to Genome." *Breeding Science* 61: 445–452.

Koester, R. P., B. M. Nohl, B. W. Diers, and E. A. Ainsworth. 2016. "Has Photosynthetic Capacity Increased with 80 years of Soybean Breeding? An Examination of Historical Soybean Cultivars." *Plant, Cell & Environment* 39: 1058–1067.

Lanigan, G. J., N. Betson, H. Griffiths, and U. Seibt. 2008. "Carbon Isotope Fractionation during Photorespiration and Carboxylation in *Senecio*." *Plant Physiology* 148: 2013–2020.

Leverett, A., and J. Kromdijk. 2024. "The Long and Tortuous Path Towards Improving Photosynthesis by Engineering Elevated Mesophyll Conductance." *Plant, Cell & Environment* 47: 3411–3427.

Li, C., E. Hoffland, T. W. Kuyper, et al. 2020. "Syndromes of Production in Intercropping Impact Yield Gains." *Nature Plants* 6: 653–660.

Liu, T., M. M. Barbour, D. Yu, S. Rao, and X. Song. 2022. "Mesophyll Conductance Exerts a Significant Limitation on Photosynthesis during Light Induction." *New Phytologist* 233: 360–372.

Liu, X., J. He, Y. Wang, et al. 2020. "Geographic Differentiation and Phylogeographic Relationships Among World Soybean Populations." *Crop Journal* 8: 260–272.

Lochocki, E. B. 2024. "PhotoGEA: Photosynthetic Gas Exchange Analysis." R package version 1.0.0". https://eloch216.github.io/PhotoGEA.

Long, S. P., A. Marshall-Colon, and X. G. Zhu. 2015. "Meeting the Global Food Demand of the Future by Engineering Crop Photosynthesis and Yield Potential." *Cell* 161: 56–66.

Long, S. P., S. H. Taylor, S. J. Burgess, et al. 2022. "Into the Shadows and Back into Sunlight: Photosynthesis in Fluctuating Light." *Annual Review of Plant Biology* 73: 617–648.

Lundgren, M. R., and A. J. Fleming. 2020. "Cellular Perspectives for Improving Mesophyll Conductance." *The Plant Journal* 101: 845–857.

Mbah, E. U., C. O. Muoneke, and D. A. Okpara. 2009. "Evaluation of Cassava *Manihot esculenta Manihot Esculenta* (Crantz) Planting Methods and Soybean *Glycine max* (L.) Merrill Sowing Dates on the Yield Performance of the Component Species in Cassava/Soybean Intercrop under the Humid Tropical Lowlands of Southeastern Nigeria." *African Journal of Biotechnology* 8: 42–47.

McAusland, L., S. Vialet-Chabrand, P. Davey, N. R. Baker, O. Brendel, and T. Lawson. 2016. "Effects of Kinetics of Light-Induced Stomatal Responses on Photosynthesis and Water-Use Efficiency." *New Phytologist* 211: 1209–1220.

Murchie, E. H., M. Pinto, and P. Horton. 2009. "Agriculture and the New Challenges for Photosynthesis Research." *New Phytologist* 181: 532–552.

Pearcy, R. W. 1990. "Sunflecks and Photosynthesis in Plant Canopies." *Annual Review of Plant Physiology and Plant Molecular Biology* 41: 421–453.

Pelech, E. A., B. C. S. Alexander, and C. J. Bernacchi. 2021. "Photosynthesis, Yield, Energy Balance, and Water-Use of Intercropped Maize and Soybean." *Plant Direct* 5, no. 12: e365.

Pelech, E. A., J. B. Evers, T. L. Pederson, D. W. Drag, P. Fu, and C. J. Bernacchi. 2023. "Leaf, Plant, to Canopy: A Mechanistic Study on Aboveground Plasticity and Plant Density Within a Maize-Soybean Intercrop System for the Midwest, USA." *Plant, Cell & Environment* 46: 405–421.

R Core Team. 2021. *R: A Language and Environment for Statistical Computing*. Vienna, Austria: R Foundation for Statistical Computing. http://www.R-project.org/.

Roeske, C. A., and M. H. O'Leary. 1984. "Carbon Isotope Effects on Enzyme-Catalyzed Carboxylation of Ribulose Bisphosphate." *Biochemistry* 23: 6275–6284.

Sakoda, K., Y. Tanaka, S. P. Long, and T. Shiraiwa. 2016. "Genetic and Physiological Diversity in the Leaf Photosynthetic Capacity of Soybean." *Crop Science* 56: 2731–2741.

Sakoda, K., W. Yamori, M. Groszmann, and J. R. Evans. 2021. "Stomatal, Mesophyll Conductance, and Biochemical Limitations to Photosynthesis during Induction." *Plant Physiology* 185: 146–160.

Salesse-Smith, C. E., S. M. Driever, and V. C. Clarke. 2022. "Modifying Mesophyll Conductance to Optimise Photosynthesis in Crops." In *Burleigh Dodds Series In Agricultural Science*, Vol. 27. Sawston, UK: Burleigh Dodds Science Publishing.

Salesse-Smith, C. E., E. B. Lochocki, L. Doran, B. E. Haas, S. S. Stutz, and S. P. Long. 2024. "Greater Mesophyll Conductance and Leaf Photosynthesis in the Field through Modified Cell Wall Porosity and Thickness via AtCGR3 Expression in Tobacco." *Plant Biotechnology Journal* 22: 2504–2517.

Soleh, M. A., Y. Tanaka, S. Y. Kim, S. C. Huber, K. Sakoda, and T. Shiraiwa. 2017. "Identification of Large Variation in the Photosynthetic Induction Response Among 37 Soybean [*Glycine max* (L.) Merr.] Genotypes That Is not Correlated with Steady-State Photosynthetic Capacity." *Photosynthesis Research* 131: 305–315.

Soleh, M. A., Y. Tanaka, Y. Nomoto, et al. 2016. "Factors Underlying Genotypic Differences in the Induction of Photosynthesis in Soybean [*Glycine max* (L.) Merr.]." *Plant, Cell & Environment* 39: 685–693.

De Souza, A. P., Y. Wang, D. J. Orr, E. Carmo-Silva, and S. P. Long. 2020. "Photosynthesis Across African Cassava Germplasm Is Limited by Rubisco and Mesophyll Conductance at Steady State, but by Stomatal Conductance in Fluctuating Light." *New Phytologist* 225: 2498–2512.

Specht, J. E., B. W. Diers, R. L. Nelson, J. F. Ferraz de Toledo, J. A. Torrion, and P. Grassini. 2014. "Soybean." In *Yield Gains in Major U.S. Field Crops*, edited by S. Smith, B. Diers, J. Specht, and B. Carver, 311–355.

Taylor, S. H., and S. P. Long. 2017. "Slow Induction of Photosynthesis on Shade to Sun Transitions in Wheat May Cost at Least 21% of Productivity." *Philosophical Transactions of the Royal Society B: Biological Sciences* 372: 20160543.

Tazoe, Y., S. VON Caemmerer, G. M. Estavillo, and J. R. Evans. 2011. "Using Tunable Diode Laser Spectroscopy to Measure Carbon Isotope Discrimination and Mesophyll Conductance to CO_2 Diffusion Dynamically at Different CO_2 Concentrations." *Plant, Cell & Environment* 34: 580–591.

Tomás, M., H. Medrano, E. Brugnoli, et al. 2014. "Variability of Mesophyll Conductance in Grapevine Cultivars under Water Stress Conditions in Relation to Leaf Anatomy and Water Use Efficiency." *Australian Journal of Grape and Wine Research* 20: 272–280.

Tomeo, N. J., and D. M. Rosenthal. 2017. "Variable Mesophyll Conductance Among Soybean Cultivars Sets a Tradeoff Between Photosynthesis and Water-Use-Efficiency." *Plant Physiology* 174: 241–257.

Ubierna, N., W. Sun, D. M. Kramer, and A. B. Cousins. 2013. "The Efficiency of C_4 Photosynthesis under Low Light Conditions in *Zea mays*, *Miscanthus* x *giganteus* and *Flaveria bidentis*." *Plant, Cell & Environment* 36: 365–381.

Wang, Y., S. J. Burgess, E. M. de Becker, and S. P. Long. 2020. "Photosynthesis in the Fleeting Shadows: an Overlooked Opportunity for Increasing Crop Productivity." *Plant Journal* 101: 874–884.

Wang, Y., S. S. Stutz, C. J. Bernacchi, R. A. Boyd, D. R. Ort, and S. P. Long. 2022. "Increased Bundle-Sheath Leakiness of CO_2 during Photosynthetic Induction Shows a Lack of Coordination between the C_4 and C_3 Cycles." *New Phytologist* 236: 1661–1675.

Warren, C. R., G. J. Ethier, N. J. Livingston, et al. 2003. "Transfer Conductance in Second Growth Douglas-Fir (*Pseudotsuga menziesii* (Mirb.)Franco) Canopies." *Plant, Cell & Environment* 26: 1215–1227.

Williams, D. R., M. Clark, G. M. Buchanan, G. F. Ficetola, C. Rondinini, and D. Tilman. 2021. "Proactive Conservation to Prevent Habitat Losses to Agricultural Expansion." *Nature Sustainability* 4: 314–322.

Supporting Information

Additional supporting information can be found online in the Supporting Information section.